Biophysical Journal Volume 77 December 1999 2953–2967

Involvement of the Carboxy-Terminus Region of the Dihydropyridine Receptor β1a Subunit in Excitation-Contraction Coupling of Skeletal Muscle

Maryline Beurg,* Chris A. Ahern,* Paola Vallejo,* Matthew W. Conklin,* Patricia A. Powers,# Ronald G. Gregg,§ and Roberto Coronado*

*Department of Physiology, University of Wisconsin School of Medicine, and #Biotechnology Center, University of Wisconsin, Madison, Wisconsin 53706; and §Department of Biochemistry, University of Louisville, Louisville, Kentucky 40202 USA

ABSTRACT Skeletal muscle knockout cells lacking the β subunit of the dihydropyridine receptor (DHPR) are devoid of slow L-type Ca^{2+} current, charge movements, and excitation-contraction coupling, despite having a normal Ca^{2+} storage capacity and Ca^{2+} spark activity. In this study we identified a specific region of the missing β1a subunit critical for the recovery of excitation-contraction. Experiments were performed in β1-null myotubes expressing deletion mutants of the skeletal muscle-specific β1a, the cardiac/brain-specific β2a, or β2a/β1a chimeras. Immunostaining was used to determine that all β constructs were expressed in these cells. We examined the Ca^{2+} conductance, charge movements, and Ca^{2+} transients measured by confocal fluo-3 fluorescence of transfected myotubes under whole-cell voltage-clamp. All constructs recovered an L-type Ca^{2+} current with a density, voltage-dependence, and kinetics of activation similar to that recovered by full-length β1a. In addition, all constructs except β2a mutants recovered charge movements with a density similar to full-length β1a. Thus, all β constructs became integrated into a skeletal-type DHPR and, except for β2a mutants, all restored functional DHPRs to the cell surface at a high density. The maximum amplitude of the Ca^{2+} transient was not affected by separate deletions of the N-terminus of β1a or the central linker region of β1a connecting two highly conserved domains. Also, replacement of the N-terminus half of β1a with that of β2a had no effect. However, deletion of 35 residues of β1a at the C-terminus produced a fivefold reduction in the maximum amplitude of the Ca^{2+} transients. A similar observation was made by deletion of the C-terminus of a chimera in which the C-terminus half was from β1a. The identified domain at the C-terminus of β1a may be responsible for colocalization of DHPRs and ryanodine receptors (RyRs), or may be required for the signal that opens the RyRs during excitation-contraction coupling. This new role of DHPR β in excitation-contraction coupling represents a cell-specific function that could not be predicted on the basis of functional expression studies in heterologous cells.

INTRODUCTION

Excitation-contraction (EC) coupling is perhaps the earliest recognized example of Ca^{2+} signaling in an excitable cell (Ebashi et al., 1969). This is a fast process in which a single action potential induces a transient elevation of cytosolic Ca^{2+}, which in turn triggers a transient shortening of the cell. EC coupling takes place at specialized junctions between transverse tubules (t-tubules) and sarcoplasmic reticulum (SR) membranes. At this location, the gap between these two membranes is minimal and key proteins are highly concentrated. Two molecular complexes colocalized across the t-tubule/SR junction are the dihydropyridine receptor (DHPR) in the t-tubule membrane and the ryanodine receptor (RyR) in the SR membrane (Block et al., 1988). The well-established paradigm of EC coupling is that in response to depolarization, the L-type Ca^{2+} channel formed by the DHPR produces a signal that briefly opens RyR channels, leading to the release of SR-stored Ca^{2+}.

DHPRs of skeletal muscle consist of α_1, α_2/δ, β, and γ subunits (Perez-Reyes and Schneider, 1994). β subunits are ~55–65-kDa proteins that bind strongly to the α_{1S} subunit at the intracellular loop between repeats I and II. Biochemical studies showed that β subunits are present as a 1:1 complex with α_{1S} and other subunits (Leung et al., 1987). The 18-amino acid motif in the I-II loop of α_1 that binds β (identified as the AID region; Pragnell et al., 1994) and the 30-amino acid motif in β that binds α_1 (identified as the BID region; De Waard et al., 1994) are highly conserved among α_1 and β subunits. The AID/BID interaction is highly specific, has an affinity in the nanomolar range, and survives membrane solubilization (Scott et al., 1997). Both the equimolar stoichiometry and the tight binding suggest α_1 and β are unlikely to separate from each other during the lifetime of the DHPR complex, although pools of free β subunits are known to be present in cells (Wicher et al., 1995). There are four β subunit genes and each produces multiple isoforms by use of alternate exons. β isoforms can be divided into five regions based on the amount of identity between them (see Fig. 1). Two highly conserved central regions (regions 2 and 4) are flanked by highly divergent N- and C-termini (regions 1 and 5) and linker regions (region 3). Region 4 contains the BID region essential for binding to the α_1 subunit (De Waard et al., 1994). Features of the primary structure (Ruth et al., 1989), biochemical data

Received for publication 30 June 1999 and in final form 18 August 1999.

Address reprint requests to Dr. Roberto Coronado, Department of Physiology, University of Wisconsin, 1300 University Ave., Madison, WI 53706. Tel.: 608-263-7487; Fax: 608-265-5512; E-mail: coronado@physiology.wisc.edu.

0006-3495/99/12/2953/15 $2.00

(Wicher et al., 1995; Scott et al., 1997), and recent predictions based on sequence homology searches (Hanlon et al., 1999), have suggested the β subunit is a peripheral membrane protein rich in secondary structure with homology domains typical of signaling proteins (SH3 domain) and receptor clustering proteins (MAGUK domain) (Craven and Bredt, 1998).

A knockout of the mouse β1 gene, encoding isoforms expressed in skeletal muscle (β1a) and brain (β1b, β1c) (Powers et al., 1992), was previously described (Gregg et al., 1996). β1-null mice die at birth due to the lack of EC coupling in the skeletal musculature. β1-null myotubes fail to contract in response to electrical stimulation despite the presence of normal action potentials, a normal Ca^{2+} storage capacity, and normal caffeine-sensitive Ca^{2+} release. β1-null cells have a low density of L-type Ca^{2+} current and charge movements and do not produce Ca^{2+} transients in response to depolarization (Strube et al., 1996, 1998). However, Ca^{2+} sparks due to the activity of ryanodine receptors are highly abundant in these cells (Conklin et al., 1999). These studies have suggested that β1-null cells fail to transduce depolarization into SR Ca^{2+} release due to one of two fundamental reasons. Either the density of DHPRs on the cell membrane of β1-null cells is too low to produce Ca^{2+} transients detectable by available techniques, or the absence of β renders membrane-located DHPRs unable to initiate EC coupling. In the former case, the EC coupling null phenotype would originate from the mistargeting of otherwise functional DHPRs. In the latter case, the null phenotype would primarily reflect an intrinsic dysfunction of the DHPR. In order to distinguish between these possibilities, we expressed different β isoforms in null cells and investigated the recovered phenotype. Expression of the skeletal muscle β1a isoform results in a quantitative recovery of the L-type Ca^{2+} current density, the intramembrane charge movement density, and the amplitude and voltage dependence of intracellular Ca^{2+} transients (Beurg et al., 1997). In contrast, expression of the nonskeletal muscle β2a isoform produced an entirely different result (Beurg et al., 1999b). β2a, like β1a, restored a Ca^{2+} current with a density, voltage-dependence, and kinetics identical to that of β1a-transfected cells. Yet β2a could not entirely restore skeletal-type EC coupling since Ca^{2+} transients evoked by voltage were significantly smaller at all potentials (Beurg et al., 1999b). These observations suggested that a unique region of β1a was required for normal EC coupling in the β1-null cell. To test this hypothesis further, we expressed several deletion mutants of β1a, β2a, and chimeric β2a-β1a isoforms. Whole-cell voltage-clamp and confocal imaging analyses showed that a quantitative recovery of the EC coupling in β1-null myotubes required a β1a isoform with an intact C-terminus. Thus a region distinct from the BID is required for the normal EC coupling function of the DHPR. Part of these results appeared in abstract form (Beurg et al., 1999a).

MATERIALS AND METHODS

Primary cultures of mouse myotubes

Primary cultures were prepared from hindlimbs of 18-day-old β1-null embryos as described elsewhere (Beurg et al., 1997). Dissected muscles were incubated for 9 min at 37°C in Ca^{2+}/Mg^{2+}-free Hanks' balanced salt solution (136.9 mM NaCl, 3 mM KCl, 0.44 mM KH_2PO_4, 0.34 mM $NaHPO_4$, 4.2 mM $NaHCO_3$, 5.5 mM glucose, pH 7.2) containing 0.25% (w/v) trypsin and 0.05% (w/v) pancreatin (Sigma, St. Louis, MO). Mononucleated cells were resuspended in plating medium containing 78% Dulbecco's modified Eagle's medium with low glucose (DMEM, Gibco BRL, Gaithersburg, MD), 10% horse serum (HS, Sigma), 10% fetal bovine serum (FBS, Sigma), 2% chicken embryo extract (CEE, Gibco), and plated on plastic culture dishes coated with gelatin at a density of $\sim 1 \times 10^4$ cells per dish. Cultures were grown at 37°C in 8% CO_2. After the fusion of myoblasts ($\sim$7 days), the medium was replaced with an FBS-free medium (88.75% DMEM, 10% horse serum, 1.25% CEE) and cells were incubated in 5% CO_2. All media contained 0.1% v/v penicillin and streptomycin (Sigma).

cDNA transfection

cDNAs were subcloned into a pSG5 expression plasmid (Stratagene, La Jolla, CA) containing the early simian virus-40 (SV40) promoter, an α1-globin intron to enhance RNA processing, and an SV40 polyadenylation signal. The original vector was modified so that 11 amino acids of the phage T7 gene 10 protein are fused to the N-terminus of the expressed β subunits. The T7 tagged-β1a subunit had a functional expression indistinguishable from the untagged β1a subunit. We also added *Age*I and *Not*I restriction enzyme sites downstream of the T7 tag to simplify cloning of the modified β subunits. Cotransfection of the pSG5 expression plasmid and a separate marker plasmid encoding the T-cell membrane antigen CD8 was performed with the polyamine LT-1 (Panvera, Madison, WI). Cotransfected cells were recognized by incubation with CD8 antibody beads (Dynal, Oslo, Norway).

cDNA constructs

Deletion and chimeric constructs of β subunits (Fig. 1) were made using PCR strategies. For deletion constructs, two oligonucleotide primers were designed to encompass the region of interest. Each primer had 20–25 bases identical to the original sequence and an additional 10–15 bases that resulted in an amplified product with an *Age*I site at the 5′ end, and a stop codon and *Not*I restriction site at the 3′ end. The PCR products were subcloned into the pCR-Blunt vector (Invitrogen Inc., Carlsbad, CA), excised by digestion with *Age*I and *Not*I and cloned into pSG5.

wt β1a

A full-length mouse β1a cDNA (amino acids 1–524) was fused in frame to the first 11 amino acids of the phage T7 gene 10 protein in the pSG5 vector.

wt β2a

A full-length rat β2a cDNA (amino acids 1–604) was fused to the first 11 amino acids of the phage T7 gene 10 protein fused in the pSG5 vector.

wt β1c

PCR primers 5′ gca tga ccg gtg gac agc aaa tgg gta tgg tcc aga aga gcg gca tgt ccc ggg gcc 3′ and 5′ gcg gcc gct agc tac cta cat ggc gtg ctc ctg agg 3′ were used to PCR a bacteriophage clone that contained the full-length mouse β1c cDNA. This cDNA was fused in frame to the first 11 amino acids of the phage T7 gene 10 protein in the pSG5 vector.

β1-3′t

PCR primers 5′ gca tga ccg gtg gac agc aaa tgg gta tgg tcc aga aga gcg gca tgt ccc ggg gcc 3′ and 5′ ggg gcg gcc gct cac tgg agg ttg gag acg ggg gca 3′ were used to generate a cDNA that contains amino acids 1–489 of the full-length mouse β1a cDNA. This cDNA was fused in frame to the first 11 amino acids of the phage T7 gene 10 protein in the pSG5 vector.

β1-5′t

PCR primers 5′ gca tga ccg gtg gac agc aaa tgg gtg gct cag cag agt cct aca c 3′ and 5′ gcg gcc gct agc tac cta cat ggc gtg ctc ctg agg 3′ were used to generate a cDNA that contains amino acids 58–524 of the full-length mouse β1a cDNA. This cDNA was fused in frame to the first 11 amino acids of the phage T7 gene 10 protein in the pSG5 vector.

β2-3′t1

A deletion of amino acids 486–600 was generated by digestion of the pSG5-T7-β2a plasmid with *Bst*XI, followed by incubation of the digested DNA with T4 DNA polymerase to chew back the 3′ overhang, digestion with *Bst*1107I and ligation of the blunt-ended linear DNA to recircularize the plasmid. The cDNA contains amino acids 1–485 fused to the N-terminus of amino acids 601–604 of the full-length rat β2a cDNA.

β2-3′t2

PCR primers 5′ gca tga ccg gtg gac agc aaa tgg gta tgc agt gct gcg ggc tgg ta 3′ and 5′ ggg ggc ggc cgc tca gtt ggg gag gtt act gct ggg a 3′ were used to generate a cDNA that contains amino acids 1–419 of the full-length rat β2a cDNA. This cDNA was fused in frame to the first 11 amino acids of the phage T7 gene 10 protein in the pSG5 vector.

Chimeric β2-β1

This construct contains amino acids 1–287 of the full-length rat β2a cDNA fused to the N-terminus of amino acids 325–524 of the full-length mouse β1a cDNA and was made by two rounds of PCR. Two primers were used to PCR the 5′ end of the full-length rat β2a cDNA, primer Rtβ2a-T7-*Age*I 5′ gca tga ccg gtg gac agc aaa tgg gta tgc agt gct gcg ggc tgg ta 3′ and primer Rtβ2a-5′chim 5′ gag cgt ttg gcc agg gag atg tca gca 3′. Two primers were used to PCR the 3′ end the full-length mouse β1a cDNA, primer Mβ1a-3′ chim 5′ tcc ctg gcc aaa cgc tcc gtc ctc aac 3′ and primer Mβ1a 3′ *Not*I 5′ gcg gcc gct agc tac cta cat ggc gtg ctc ctg agg 3′. The primers were designed to produce two PCR products with a 17-bp overlap of identical sequence. The two PCR products were electrophoresed on agarose gels, excised from the gel, and eluted using GenElute columns (SupelCo, Bellefonte, PA). The two PCR products were mixed in an equimolar ratio, denatured, allowed to reanneal, and used in a PCR reaction to amplify the chimeric fragments using Rtβ2a-T7-*Age*I and Mβ1a 3′ *Not*I primers. This cDNA was fused in frame to the first 11 amino acids of the phage T7 gene 10 protein in the pSG5 vector.

β2-β1-3′t

PCR primers 5′ gca tga ccg gtg gac agc aaa tgg gta tgc agt gct gcg ggc tgg ta 3′ and 5′ gcg gcc gct agc tac cta cat ggc gtg ctc ctg agg 3′ were used to generate a 3′ truncated chimeric cDNA. This cDNA contains amino acids 1–287 of the full-length rat β2a cDNA fused to the N-terminus of amino acids 325–464 of the full-length mouse β1a cDNA. The cDNA was fused in frame to the first 11 amino acids of the phage T7 gene 10 protein in the pSG5 vector.

Ca^{2+} current and charge movements

Whole-cell recordings were performed as described previously (Strube et al., 1996) with an Axopatch 200B amplifier (Axon Instruments, Foster City, CA). Linear capacitance and leak currents were compensated with the circuit provided by the manufacturer. Effective series resistance was compensated up to the point of amplifier oscillation with the Axopatch circuit. All experiments were performed at room temperature. The external solution was (in mM) 130 TEA methanesulfonate, 10 $CaCl_2$, 1 $MgCl_2$, 10^{-3} TTX, and 10 HEPES titrated with TEA(OH) to pH 7.4. The pipette solution consisted of (in mM) 140 cesium aspartate, 5 $MgCl_2$, 0.1 EGTA (when Ca^{2+} transients were recorded), or 5 EGTA (all other recordings), and 10 MOPS titrated with CsOH to pH 7.2. Patch pipettes had a resistance of 2–5 MΩ when filled with the pipette solution. For recordings of charge movement, the external solution was supplemented with 0.5 mM $CdCl_2$ and 0.1 mM $LaCl_3$ to block the ionic Ca^{2+} currents. A prepulse protocol previously described (Beurg et al., 1999b) was used to measure the immobilization-resistant component of charge movement. Voltage was first stepped up from holding potential −80 mV to −20 mV for 1 s, then to −50 mV for 5 ms, then to test potential *P* for 25 ms, then to −50 mV for 30 ms and finally to the −80 mV holding potential. Subtraction of linear components was assisted by a *P*/4 procedure following the pulse paradigm listed above. *P*/4 pulses were in the negative direction, had a duration of 25 ms, and were separated by 500 ms.

Confocal fluorescence microscopy

Confocal line-scan measurements were performed as described elsewhere (Conklin et al., 1999). Cells were loaded with 4 μM fluo-3 acetoxymethyl (AM) ester (Molecular Probes, Eugene, OR) for 20 to 40 min at room temperature. A 1-mg sample of fluo-3 AM (Molecular Probes) was dissolved in 1 ml DMSO and kept frozen until use. All experiments were performed at room temperature. Cells were viewed with an inverted Olympus microscope with a 20× objective (N.A. = 0.4) and an Olympus Fluoview confocal attachment (Melville, NY). The 488-nm spectrum line necessary for fluo-3 excitation was provided by a 5 mW argon laser attenuated to 20% with neutral density filters. The fluorescence intensity, *F*, was calculated by densitometric scanning of line-scan images and was averaged over the entire width of the cell. The fluorescence intensity *Fo* was averaged in the same manner from areas of the same image before the voltage pulse.

Immunostaining

Cells were transfected with T7-tagged β constructs for four days and later fixed in 100% methanol and processed for immunostaining as previously described (Gregg et al., 1996). The primary antibody was a mouse monoclonal against the T7 epitope (Novagen, Madison, WI) and was used at a dilution of 1:1000. The secondary antibody was a fluorescein conjugated polyclonal goat anti-mouse IgG (Boehringer Mannheim, Indianapolis, IN) and was used at a dilution of 1:1000. Confocal images of 1024 × 1024 pixels (0.35 μm/pixel) were obtained in the Olympus Fluoview using the 488-nm spectral line for dye excitation and a 40× oil-immersion objective (N.A. 1.3) for capturing emission. Images were Kalman-averaged three times and the pixel intensity displayed as 16 levels of gray in reverse. All images were acquired using minimal laser power (6% of maximum 5 mW) and predetermined PMT settings to avoid pixel saturation and for accuracy in the comparison of images.

Curve-fitting

For each cell the voltage-dependence of charge movements (*Q*), Ca^{2+} conductance (*G*), and peak intracellular Ca^{2+} ($\Delta F/F$) was fitted according to a Boltzmann distribution

$$A = A_{max}/(1 + \exp(-(V - V_{1/2})/k)). \quad (1)$$

Where A_{max} was either Q_{max}, G_{max}, or $\Delta F/F_{max}$, $V_{1/2}$ is the potential at which $A = A_{max}/2$, and k is the slope factor. The time constant, τ_1, describing activation of the Ca^{2+} current was obtained from a fit of the pulse current at each voltage according to

$$I(t) = K[1 - (\exp - t/\tau_1)]\exp - t/\tau_2 \quad (2)$$

Where K is constant and τ_2 describes inactivation. Parameters from a fit of separate cells are shown in Table 1. Parameters from a fit of averages of many cells (population averages) are shown in Figs. 4, 6, and 8.

cDNA sequencing

All β constructs were sequenced before their use in experiments at the Biotechnology Center, University of Wisconsin.

RESULTS

The β subunits analyzed in this study are shown in Fig. 1. Sequence comparison between the full-length β1a and β2a isoforms revealed two highly conserved central regions (regions 2 and 4), a nonconserved linker region between the two conserved domains, and distinct N- and C-termini. We tested the participation of the nonconserved regions 1, 3, and 5 of β1a in the recovery of Ca^{2+} conductance, charge movements, and EC coupling in β1-null cells. These regions were respectively deleted in constructs β1-5′t, the splice-variant β1c (Powers et al., 1992), and β1-3′t. In addition, we tested region 5 of β2a (constructs β2-3′t and β2-3t2) and region 5 of a chimera composed of an N-terminus half of β2a and a C-terminus half of β1a (constructs β2-β1 and β2-β1-3′t). Measurements were made in whole-cell voltage-clamped myotubes at day 8 to 12 after cDNA transfection. We previously showed that within this period, the Ca^{2+} conductance of transfected β1-null cells remains relatively constant (Beurg et al., 1997). Therefore, a precise synchronization of cell cultures was not required for a quantitative comparison of the functional expression of DHPRs in different batches of transfected cells. All transfected β constructs carried an 11-amino acid T7 tag at the N-terminus, which was first tested in the wt β1a cDNA and was found not to interfere with function. This epitope was useful for determining whether a given construct was expressed in β1-null cells.

Fig. 2 shows close-up confocal views of myotubes fixed and immunostained with T7 antibody and a fluorescein-conjugated secondary antibody. There was abundant expression of each of the tested constructs throughout the length of myotubes, and in many cases expression was heavily concentrated in the cell periphery. The latter is consistent with the known location of DHPRs in the periphery of cultured myotubes where couplings are established between the plasma membrane and the sarcoplasmic reticulum membrane (Takekura et al., 1994). The CD8 cDNA was used as a transfection marker and micron-size beads, with absorbed CD8 antibody, were used to identify transfected cells (see asterisks). Better than 95% of cells expressing CD8 also expressed β as determined from the coincidence of the T7 immunostain and CD8 beads in a given cell and the coincidence of CD8 beads and a high density of L-type Ca^{2+} current in a given cell.

Fig. 3 shows the L-type Ca^{2+} currents of cells transfected with each of the tested β constructs in response to the pulse potentials indicated in the top left set of traces. Each whole-cell clamped myotube was subjected to a total of 20 voltage pulses of increasing amplitude and a constant duration of 300 ms starting from a holding potential of −40 mV. For ease of comparison, only four traces of currents are shown in each case. Currents have been normalized according to the cell capacitance. The current scale is the same for all cells except for the two cells expressing the chimeric β2-β1 constructs. The Ca^{2+} current recovered by the constructs had a threshold for activation more positive than −30 mV, had remarkably slow activation kinetics, and a fast deactivation. These features are entirely consistent with the known properties of skeletal L-type Ca^{2+} currents of control (wt) mouse myotubes in cell culture (Garcia et al., 1994a; Beurg et al., 1997). These features contrast with those of Iβ-null, the Ca^{2+} current of nontransfected β1-null myotubes, which is much faster and has a significantly lower density (Beurg et al., 1997; Strube et al., 1998).

The voltage-dependence of the Ca^{2+} conductance recovered by each of the tested constructs is shown in Fig. 4. The Ca^{2+} conductance was estimated from the extrapolated reversal potential and the end-pulse current in each of the 20

TABLE 1 Parameters of the Ca^{2+} conductance, charge movement, and Ca^{2+} transient expressed by β constructs in β1-null myotubes

	G-V Curve (Ca)			*Q-V* Curve			$\Delta F/Fo/V$-Curve		
	G_{max} (pS/pF)	$V_{1/2}$ (mV)	k (mV)	Q_{max} (nC/μF)	$V_{1/2}$ (mV)	k (mV)	$\Delta F/Fo_{max}$	$V_{1/2}$ (mV)	k (mV)
β1a	161.2 ± 6.9 (9)	14.5 ± 1.8	4.9 ± 0.2	6.8 ± 0.9 (6)	19 ± 2.5	14.7 ± 1.6	3.3 ± 0.5 (9)	5 ± 4.5	8.1 ± 1.7
β1c	169 ± 21.3 (12)	9 ± 1.2	4.2 ± 0.4	5 ± 0.8 (7)	19.5 ± 2.3	11.7 ± 0.9	3.3 ± 0.4 (11)	−3.4 ± 0.2	5.8 ± 0.7
β1a-3′t	87.8 ± 7.4 (15)	20.5 ± 1.1	5.2 ± 0.2	6.4 ± 1.3 (5)	20.2 ± 1.8	11 ± 1.4	0.65 ± 0.1 (7)	3 ± 2	9 ± 4
β1a-5′t	164.5 ± 7.8 (10)	15.8 ± 2.1	5.0 ± 0.2	5.9 ± 1 (5)	21.5 ± 2.2	12 ± 0.5	1.9 ± 0.5 (6)	−1.4 ± 4	8.8 ± 1.9
β2a	152.7 ± 12 (15)	10.4 ± 0.8	5.2 ± 0.3	2.6 ± 0.2 (11)	16.7 ± 2.4	15 ± 1.3	1.1 ± 0.2 (7)	0.6 ± 3.5	5.6 ± 1.7
β2a-3′t	149 ± 13.8 (10)	14 ± 1.5	5.2 ± 0.2	4.9 ± 0.4 (7)	19 ± 2.7	15.2 ± 0.8	2.0 ± 0.6 (4)	0.7 ± 2	5.7 ± 0.7
β2a-3′t2	137.2 ± 9.3 (12)	20.6 ± 1.7	4.7 ± 0.3	4 ± 0.3 (5)	22 ± 2.2	11 ± 0.9	0.9 ± 0.4 (6)	7.5 ± 3.4	10.1 ± 2.6
β2-β1	319.6 ± 3.8 (11)	16.8 ± 1.7	4.8 ± 0.4	5.1 ± 0.5 (7)	22.5 ± 2.1	11.5 ± 1.2	3.8 ± 0.7 (7)	−3.7 ± 3.1	6.7 ± 2.3
β2-β1-3′t	160.3 ± 5.7 (14)	18.6 ± 1.4	5.0 ± 0.2	3.8 ± 0.3 (5)	20.2 ± 3.6	10.3 ± 1	1.4 ± 0.4 (10)	3.5 ± 2.3	5.5 ± 0.9

Entries (mean ± SE) correspond to Boltzmann parameters fitted separately to each cell. The number of cells is shown in parentheses.

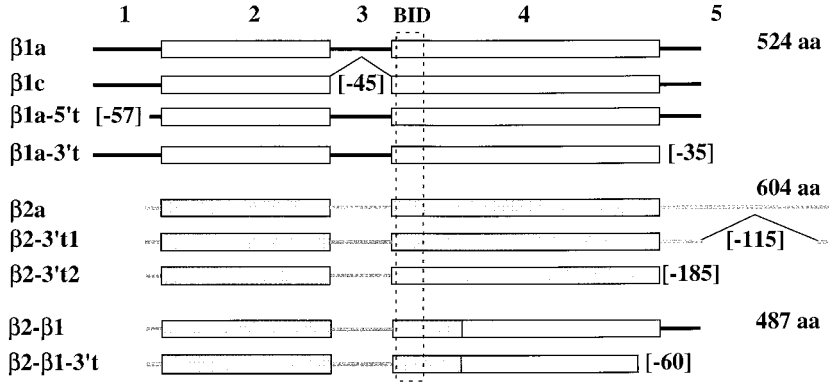

FIGURE 1 Alignment to scale of the amino acid sequence of the tested β constructs. The boxes indicate conserved domains described elsewhere (Perez-Reyes and Schneider, 1994). The amino acid coordinates of each construct are indicated in Materials and Methods.

300-ms pulses. The curves are a Boltzmann fit of the population mean with parameters indicated in the figure legend. The curve without symbols corresponds to the conductance of nontransfected cells obtained in a previous study (Beurg et al., 1997). In addition to these data, the Boltzmann parameters of the Ca^{2+} conductance averaged for 9 to 15 cells in each case are shown in Table 1. In Fig. 4 *A* we examined *G-V* curves of cells expressing deletion constructs of the β1a isoform. Deletion of region 3 between the two conserved domains (construct β1c) or deletion of almost the entire region 1 (construct β1-5′t) had no effect on the recovered maximum Ca^{2+} conductance, which for these constructs and for wt β1a was ~160 pS/pF. However, the deletion of region 5 (construct β1-3′t) resulted in a 1.8-fold (161/88) reduction in the recovered maximum Ca^{2+} conductance that was statistically significant (unpaired *t*-test with $p = 0.0001$). Scaled *G-V* curves of cells expressing β1-3′t and wt β1a are shown in Fig. 4 *A, top*. The 3′ truncation had no effect of the steepness of the *G-V* curve, although it produced an ~5 mV positive shift, which according to an unpaired *t*-test was not significant. In Fig. 4 *B* we examined whether a 3′ truncation of β2a, which in full-length was shown to express skeletal L-type Ca^{2+} currents at a density similar to that of control (wt) myotubes (Beurg et al., 1999b), also curtailed the expressed Ca^{2+} current density. A partial deletion of region 5 of β2a (construct β2-3′t) or a complete deletion of the 185 residues encompassing region 5 of β2a (construct β2-3′t2) had no effect on the maximum Ca^{2+} conductance or the steepness of the *G-V* curve (unpaired *t*-tests with $p > 0.8$). Both parameters were similar to those of cells expressing β1a (Table 1). However, the more severe β2-3′t2 truncation produced an ~10 mV positive shift of the *G-V* curve, shown in Fig. 4 *B, top*, that was statistically significant (unpaired *t*-test with $p < 0.04$). In Fig. 4 *C* we examined the voltage-dependence of the Ca^{2+} conductance produced by the β2-β1 chimera and the 3′ truncated chimera. The "full-length" chimera expressed a remarkably large specific Ca^{2+} conductance of ~320 pS/pF or twice that of wt β1a or wt β2a. Truncation of the 3′ end of this chimera, encompassing the entire region 5 of β1a, resulted in a twofold (320/160) reduction in Ca^{2+} conductance that was highly significant (unpaired *t*-test with $p = 0.001$). The scaled *G-V* relationships shown in Fig. 4 *C, top* revealed that the steepness and midpoints of both curves did not change. In summary, the expression of wt β1a or wt β2a in β1-null cells restored a Ca^{2+} current with a density typical of normal (wt) myotubes (Beurg et al., 1997). The voltage-dependence of the Ca^{2+} currents strongly suggests these must have originated from complexes of β, α_{1S}, and the other subunits of the skeletal DHPR complex. A deletion of the nonconserved region 5 of β1a, but not regions 1 or 3, resulted in a significant reduction of the expressed Ca^{2+} current. This reduction was specific for region 5 of β1a as demonstrated by deletion approaches using wt β2a and the β2-β1 chimera.

The kinetics of activation of the Ca^{2+} current of skeletal muscle is the slowest among voltage-gated Ca^{2+} channels, and this characteristic is determined in part by repeat I of the α_{1S} subunit (Tanabe et al., 1991). Therefore, the kinetics of the Ca^{2+} current recovered in β1-null cells should provide critical information on whether the expressed β subunits rescued a skeletal-type DHPR. In these experiments we used a 1.5-s depolarizing pulse from a holding potential of −40 mV to fit the activation and inactivation phases of the Ca^{2+} current. However, none of the constructs altered the inactivation rate to any great extent and in all cases the peak current inactivated <20% at the end of this relatively long pulse. The pulse current was fitted with Eq. 2, which conforms to a linear kinetic scheme with closed, open, and inactive states and assumes that for a sufficiently long pulse, inactivation is complete. Because pulses longer than 1.5 s invariably resulted in a loss of the pipette seal, this assumption could not be verified. In all cases we found an excellent agreement between the fit and the pulse current as previously shown for β1-null cells expressing wt β1a or wt β2a (Beurg et al., 1997, 1999b).

Fig. 5 shows the time constant of activation, τ_1 of Eq. 2, fitted to the Ca^{2+} current recovered by each β construct at positive potentials. In this range of potentials, the activation rate of the recovered Ca^{2+} currents slowed for increasingly positive potentials by a factor of ~2, which is characteristic of the slow skeletal L-type Ca^{2+} channel (Strube et al., 1996; Dirksen and Beam, 1995). Data are shown for each of the constructs labeled with the same symbols as in the previous figures. With two exceptions, the activation time constant of any two β constructs within each panel (*A–C*) in

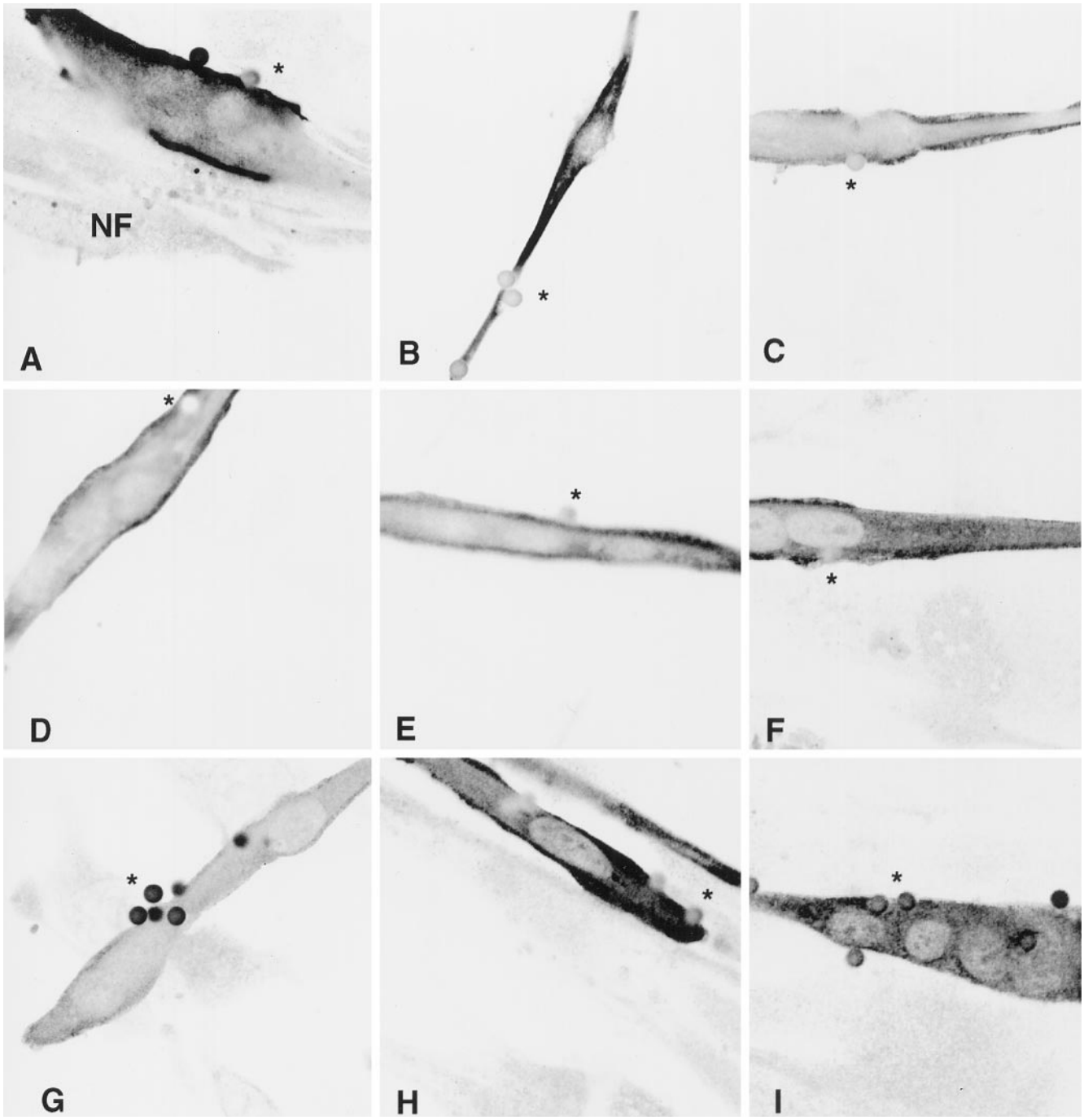

FIGURE 2 Immunofluorescence of β1-null myotubes coexpressing a T7 tagged β construct. Cells transfected with T7 tagged constructs and CD8 cDNA were incubated with CD8 antibody beads, fixed, and stained with T7 primary/fluorescein-conjugated secondary antibodies. Confocal images of 1024 $\times$ 1024 pixels (360 $\times$ 360 μm) were converted to a 16-level inverted gray scale so that high-intensity pixels appear black and low-intensity pixels appear white. Asterisks indicate some CD8 antibody beads bound to cotransfected cells. NF indicates nontransfected myotubes in the same field of β1a transfected cells (*A*). Other panels show expression of T7 tagged β1c (*B*), β1-5′t (*C*), β1-3′t (*D*), β2a (*E*), β2-3′t (*F*), β2-3′t2 (*G*), β2-β1 (*H*), and β2-β1-3′t (*I*).

Fig. 5 were not significantly different at any test potential. One exception was the activation of β1a-3′t (*black triangles*), which at +30, +40, or +50 mV was slightly faster than that of wt β1a (*black circles*) or the other β constructs according to unpaired *t*-tests at each voltage ($p < 0.05$). The other was the activation of β2a-3′t (*white squares*) which at +10, +20, +30, or +40 mV was slightly slower than that of wt β2a (*white circles*) ($p < 0.04$). The activation time constants for all constructs, except for β1a-3′t and β2a-3′t, averaged 50 to 70 ms at +30 mV. These values agreed with previous determinations in normal myotubes (Strube et al., 1996) and in myotubes expressing chimeras of α_{1S} and α_{1C} when repeat I was from α_{1S} (Tanabe et al., 1991). The slow activation observed in cells transfected with β constructs

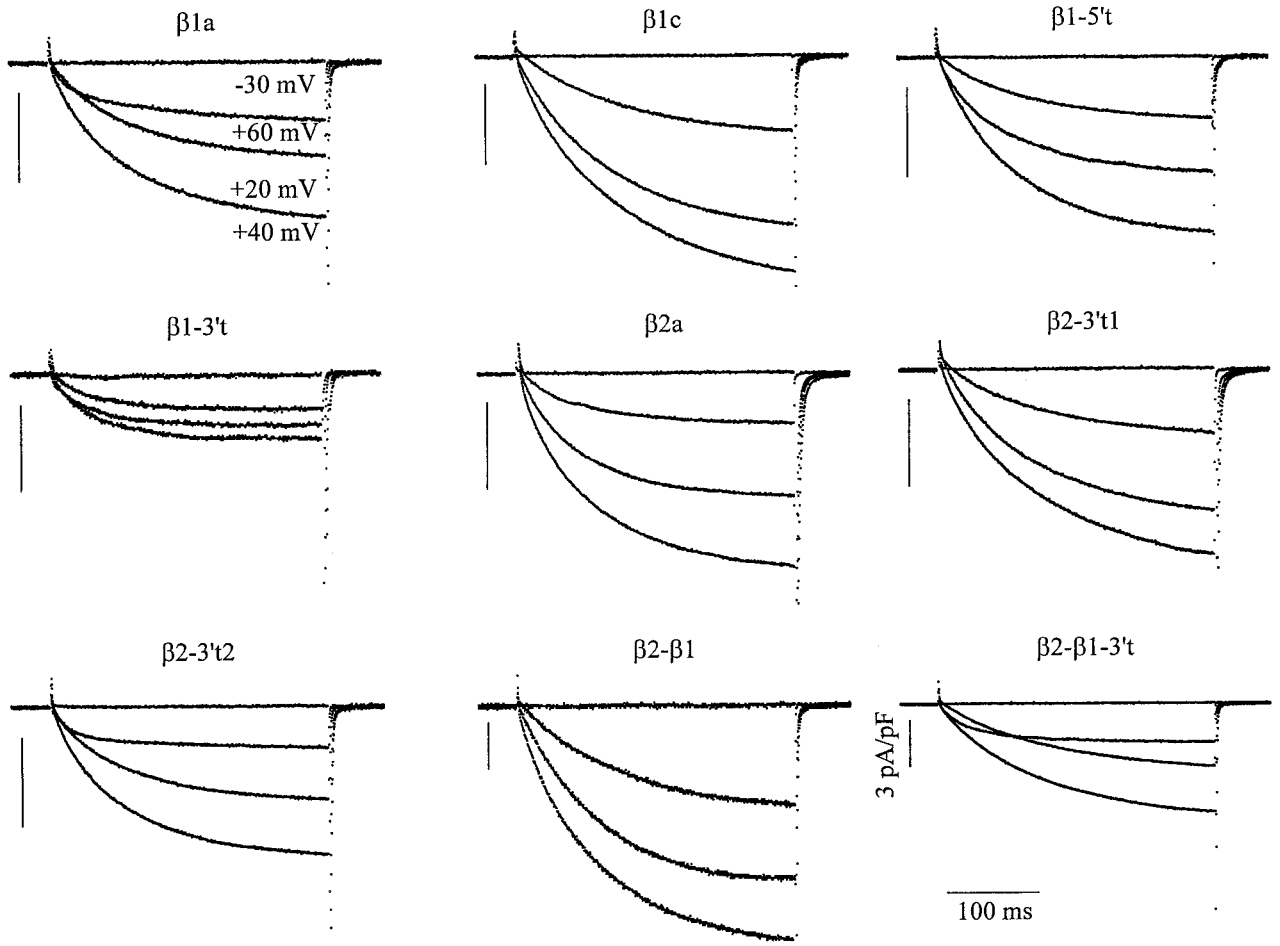

FIGURE 3 Traces of Ca^{2+} currents are from the same β1-null cell expressing the indicated β construct. The pulse duration was 300 ms and the holding potential was −40 mV. The vertical scale is 3pA/pF in all cases.

suggested that all β constructs formed complexes with α_{1S}, rather than with α_{1C}-type isoforms that could potentially be expressed in the myotube (Chaudhari and Beam, 1993; Pereon et al., 1997). We also compared the inactivation time constant, τ_2 of Eq. 2. The inactivation time constant, fitted with the limitation of the pulse duration discussed above, was 4.5 ± 1.3 s for cells expressing β1a, 4.5 ± 0.67 s for cells expressing β2a, and 4.8 ± 0.5 s for cells expressing the β2-β1 chimera. Thus, notwithstanding the two exceptions described above that produced mild changes in activation kinetics, the main conclusion from these experiments was that the kinetics of activation and perhaps also that of inactivation of the L-type Ca^{2+} current rescued by β constructs in β1-null cells was either weakly modified or not modified at all by β constructs.

The bulk of the immobilization-resistant nonlinear charge movements in myotubes in culture originates from DHPRs that include the α_{1S} subunit (Adams et al., 1990). These DHPR-mediated charge movements are directly responsible for the restoration in dysgenic (α_{1S}-null) myotubes of skeletal-type EC coupling (Tanabe et al., 1990). Both observations have strongly suggested that charge movements provide a critical index of the density of functional DHPRs that is independent of whether these DHPRs function as L-type Ca^{2+} channels. Here we measured the immobilization-resistant charge movements with a pulse of 20 ms and a protocol design to minimize contamination by the Na^+ channel gating current and ionic current (Strube et al., 1996). Charge movements were calculated by integration of the ON component on the nonlinear capacitance after verification that ON and OFF components differed by 20% or less.

Fig. 6 shows population average *Q-V* relationships for the tested β constructs. Cells were rejected unless the ON and OFF components agreed within 20%. The curves correspond to a Boltzmann fit of the population average *Q-V* curves with parameters indicated in the figure legend. The curve without symbols corresponds to the mean charge movements of nontransfected β1-null cells obtained in a previous study using the same pulse protocol (Beurg et al., 1997). Averages of Boltzmann parameters fitted separately to each cell are shown in Table 1. The onset of charge movements occurred at ~−10 mV and increased with voltage until a plateau was reached at potentials more positive than +40 mV. Fig. 6 *A* shows *Q-V* relationships of cells

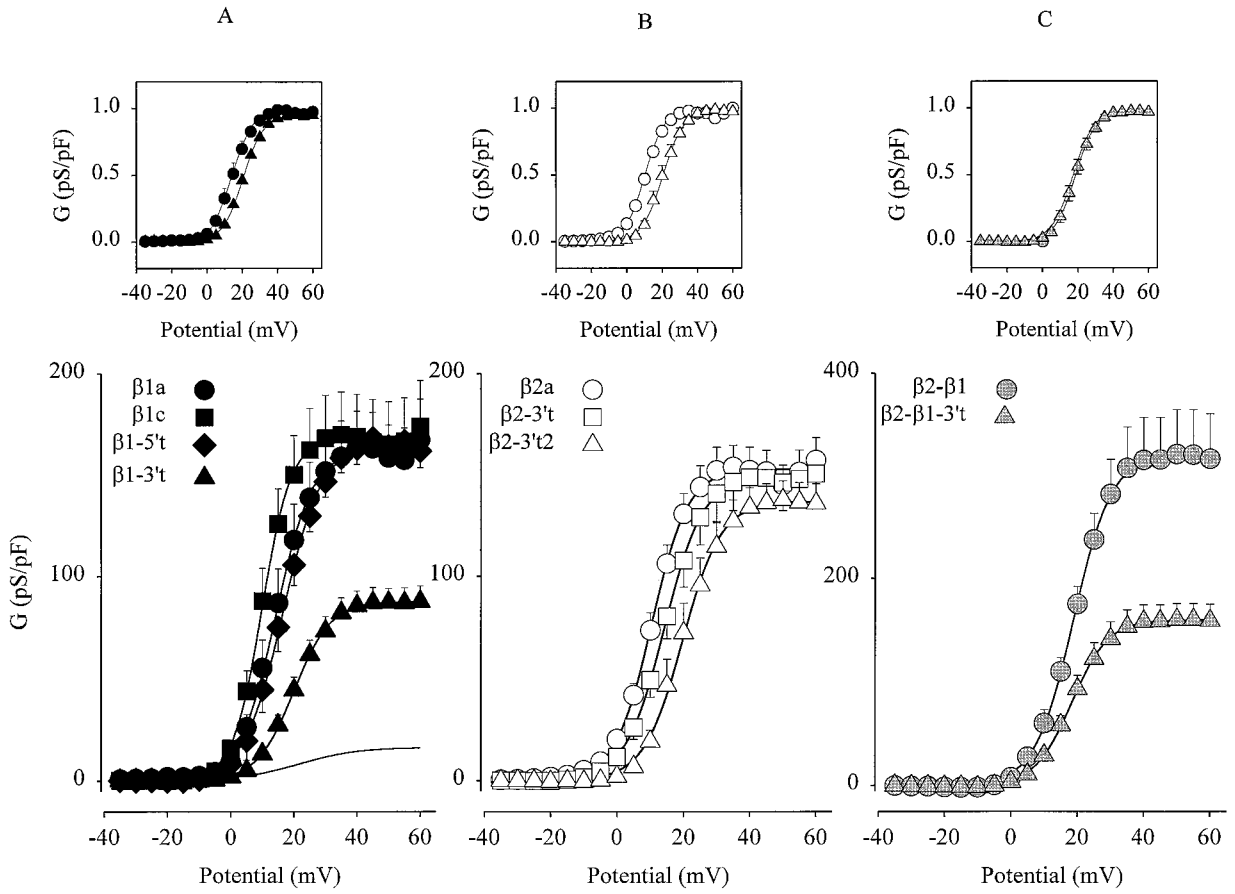

FIGURE 4 Voltage-dependence of the population average Ca^{2+} conductance in (*A*) β1a (n = 9), β1c (n = 12), β1-5′t (n = 10), and β1-3′t (n = 15); (*B*) in β2a (n = 15), β2-3′t (n = 10), β2-3′t2 (n = 12); and (*C*) β2-β1 (n = 11) and β2-β1-3′t (n = 14) transfected myotubes. The curve without symbols represents the Boltzmann fit of *G-V* curve of nontransfected cells (G_{max} = 16.2 pS/pF; $V_{1/2}$ = 21.5 mV, and k = 9.4 mV). Curves correspond to a Boltzmann fit of the population mean *G-V* curve. Parameters of the fit were in (*A*) G_{max} = 162.3, 168.5, 165.5, 87.6 pS/pF; $V_{1/2}$ = 14.2, 9.9, 16.6, 20 mV, and k = 5.7, 4.6, 6.1, 5.8 mV for β1a, β1c, β1-5′t, and β1-3′t, respectively; (*B*) G_{max} = 152.7, 149, 136.8 pS/pF; $V_{1/2}$ = 10.4, 14.2, 19.7 mV and k = 5.4, 5.8, 5.8 mV for β2a, β2-3′t, β2-3′t2; and (*C*) G_{max} = 320.8, 159.8 pS/pF; $V_{1/2}$ = 18.8, 18.3 mV and k = 5.7, 5.5 mV for β2-β1 and β2-β1-3′t transfected cells, respectively. The top panels show the conductance normalized according to the mean maximum (G_{max}) of each group of cells.

expressing deletions mutants of β1a. In all cases, the maximum charge movements, Q_{max}, were significantly larger than the Q_{max} of nontransfected cells, which averaged 2.5 ± 0.2 nC/μF (Beurg et al., 1997). This result indicated a robust recovery of membrane-associated DHPRs by the β1 constructs. The Q_{max} of cells expressing wt β1a was ~6.5 nC/μF, a value that agreed with determinations in normal (wt) myotubes and in α_{1S}-transfected dysgenic myotubes (Garcia et al., 1994a; Strube et al., 1996; Beurg et al., 1997). In addition, the Q_{max} of cells expressing β1-3′t or β1-5′t was not significantly different from that of cells expressing wt β1a. Furthermore, neither the midpoint nor the steepness of these *Q-V* curves was significantly different (see Table 1). However, the Q_{max} of cells expressing β1c was the lowest for this group of constructs, yet the difference between β1c and wt β1a (5 ± 0.8 vs. 6.8 ± 0.9 nC/μF, respectively) was not significant (p = 0.08).

The results of Fig. 6 *A* clearly demonstrated that the lower Ca^{2+} conductance of cells expressing the 3′-truncated β1 subunit could not be explained by a lower density of membrane-associated DHPRs recovered by this construct. In Fig. 6 *B* we examined the charge movements produced by the truncated β2a constructs. The Q_{max} of cells expressing wt β2a was much lower than that of wt β1a-expressing cells and, in fact, indistinguishable from that of nontransfected cells. Although this result agreed with a previous determination (Beurg et al., 1999b), it is a puzzling one because the density of the Ca^{2+} currents recovered by wt β2a was similar to that recovered by wt β1a (see Fig. 4 and Table 1). The previous study showed that the same difference in Q_{max} between β1a and β2a expressing cells was measured from a more negative holding potential (−120 mV), indicating that the low Q_{max} of β2a expressing cells was not due to a selective immobilization of charge produced by β2a (Beurg et al., 1999b). We thus surmise that the charge movements associated with the opening of β2a-recovered Ca^{2+} channels must have been masked by the background charge movements present in the β1-null myotube. Quite surprisingly, Fig. 6 *B* shows that the C-terminus deletion mutants β2-3′t and β2-3′t2 expressed charge movements signifi-

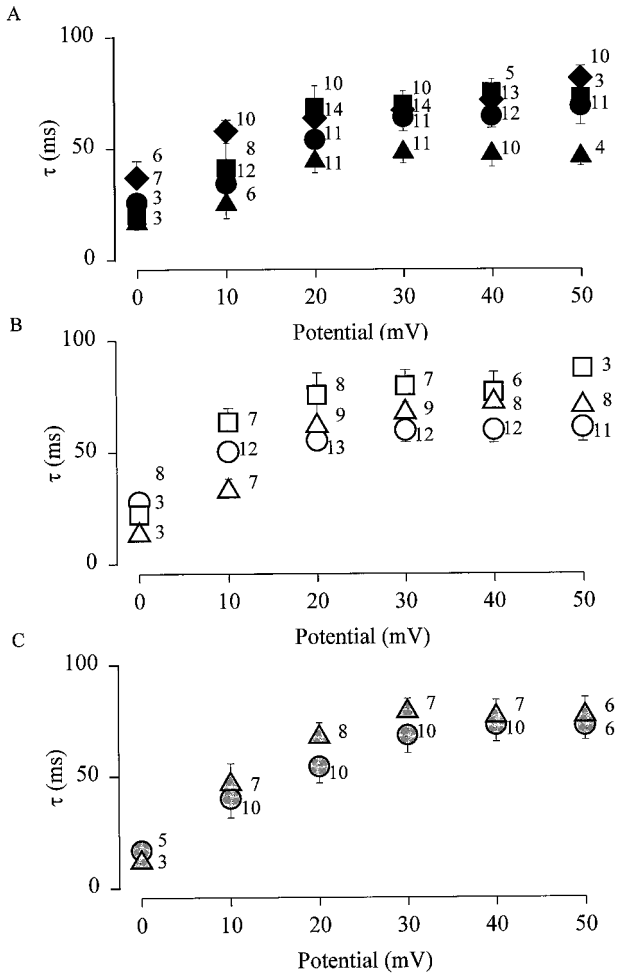

FIGURE 5 Voltage-dependence of the time constant of activation $\tau 1$ (mean ± SE) obtained from the fit in Eq. 2 for the indicated number of cells. The symbols represent the same cell types shown in all figures (see Fig. 4).

cantly higher than those of the full-length construct. Table 1 shows that in the case of β2-3′t there was a statistically significant (unpaired *t*-test with $p = 0.00001$) doubling of the Q_{max} from 2.6 ± 0.2 nC/μF produced by wt β2a to 4.9 ± 0.4 nC/μF produced by the 3′ truncated β2a. This result is in contrast with the identical Ca^{2+} conductance produced by both constructs (Table 1), which were 152.7 ± 12 pS/pF and 149 ± 13.8 pS/pF, respectively. A complete deletion of region 5 (construct β2-3′t2) produce a 1.5-fold increase in Q_{max} that also was highly significant ($p = 0.0008$). Both results clearly indicated that the C-terminus of β2a interfered with the expression of DHPR charge movements. Furthermore, the recovery of charge movements without a concomitant recovery of L-type Ca^{2+} current indicated that in the DHPR these two events, namely voltage-induced movements of electrical charges and opening the Ca^{2+} channel, are not uniquely associated. In Fig. 6 *C* we examined the charge movements produced by the β2-β1 chimera and its 3′ truncated form. The Q_{max} produced by this chimera was closer to that produced by wt β1a than to that produced by wt β2. The truncation slightly reduced the Q_{max}, although the difference was not statistically significant (unpaired *t*-test with $p = 0.4$). In summary, all β constructs except wt β2a recovered saturable movements of charge with a maximum density significantly higher than the background charge movements of nontransfected cells. Thus, except for wt β2a, all β constructs recovered electrically detectable amounts of membrane-associated DHPRs. A Boltzmann fit of the *Q-V* relationships (Table 1) showed that 1) the midpoints were not modified by the tested β isoforms; 2) the steepness factor was modestly affected; 3) the Q_{max} produced by deletion mutants of β1a were not affected; 4) the Q_{max} produced by the C-terminus truncated β2a constructs was increased; and 5) there was no unique correlation between the density of expressed charge movements and the density of expressed Ca^{2+} currents in any of the three groups (*panels A–C*) of β isoforms tested.

The contribution of the expressed β constructs to EC coupling was examined by measurements of intracellular Ca^{2+} using confocal line-scan imaging of fluo-3 fluorescence. Transfected cells were loaded with the cell-permeant form of fluo-3 and were whole-cell voltage-clamped. In some nontransfected cells slowly evolving Ca^{2+} "waves" could be evoked by depolarization from −80 mV that were presumably due to Ca^{2+}-induced Ca^{2+} release produced by Ca^{2+} entry via T-type channels (not shown). To avoid the contribution of the T-type current, the holding potential was set at −40 mV (Strube et al., 1996). Extensive controls (15 of 15 cells) convinced us that no changes in cytosolic Ca^{2+} occurred in nontransfected β1-null cells from this holding potential.

Fig. 7 shows Ca^{2+} transients in cells expressing the indicated β constructs stimulated by a 50-ms depolarization to +70 mV from −40 mV. In the line-scan images time increases from left to right. The depolarizing pulse was delivered 100 ms after the start of the line scan as indicated in the bottom of the figure. The line-scan direction was in most instances across the myotube width rather than parallel to the length of the myotube. The magnification was the same in all cases and was adjusted so that the top and bottom borders of the line-scan image would roughly correspond with the edges of the cell. Also, the laser power, photomultiplier gain, and pixel size were kept constant to minimize errors when comparing the fluorescence of different cells. The traces under each image correspond to the fluorescence in $\Delta F/F$ units averaged across the entire line-scan. Ca^{2+} release started at the onset of the depolarization and peaked at ~100 ms in all cases. The decay phase of the transient outlasted the depolarization by a significant amount of time, in agreement with studies in normal rat and mouse myotubes in culture (Garcia and Beam, 1994b; Beurg et al., 1997, 1999b). The peak fluorescence was in excess of four $\Delta F/F$ for cells expressing the endogenous wt β1a construct and for cells expressing the β2-β1 chimera. In both cases, the C-terminus truncation resulted in a dramatic decease in the peak fluorescence to <2 $\Delta F/F$ units. However, cells expressing wt β2a produced a modest Ca^{2+} transient that increased when this isoform was truncated.

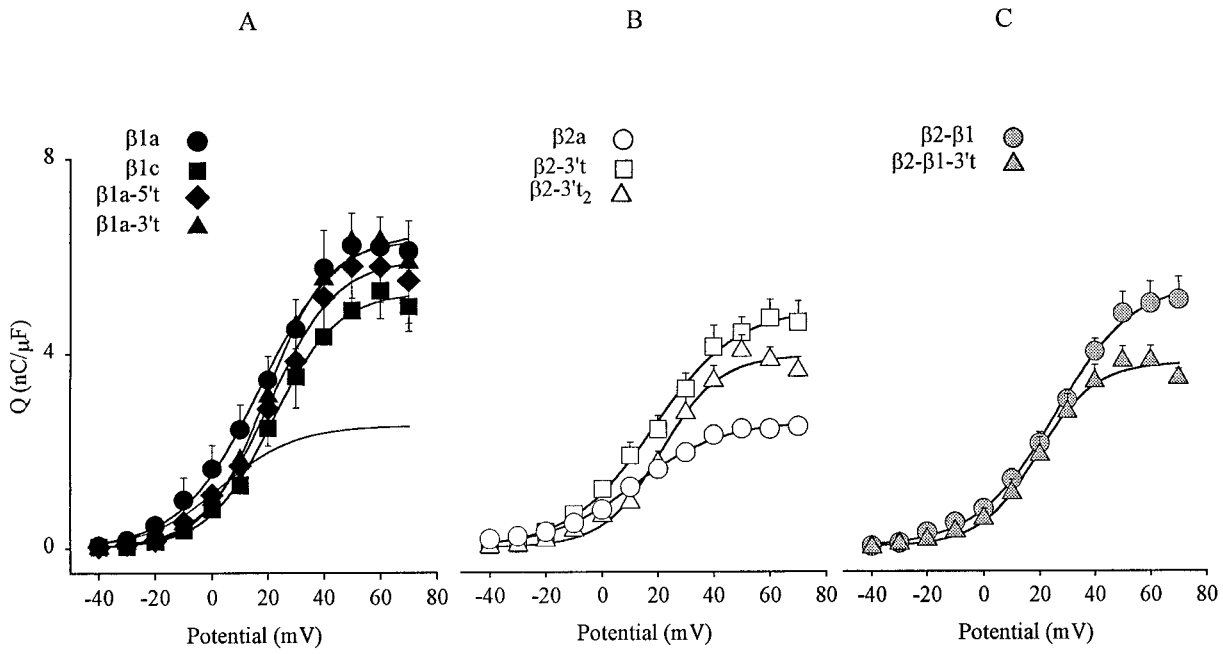

FIGURE 6 Voltage-dependence of immobilization-resistant charge movements (mean ± SE) in β1a ($n = 6$), β1c ($n = 7$), β1-5′t ($n = 5$), and β1-3′t ($n = 5$); (*B*) in β2a ($n = 11$), β2-3′t ($n = 7$), β2-3′t2 ($n = 5$); and (*C*) β2-β1 ($n = 7$) and β2-β1-3′t ($n = 5$) transfected myotubes. Curves correspond to a Boltzmann fit of the population mean *Q-V* curve. Parameters of the fit are (*A*) $Q_{max} = 6.5, 5.3, 5.9, 6.3$ nC/μF; $V_{1/2} = 16.9, 21.8, 20.6, 19.6$ mV; $k = 13.9, 11.5, 11.9, 10.7$ mV for β1a, β1c, β1-5′t and β1-3′t, respectively; (*B*) $Q_{max} = 2.6, 4.9, 3.9$ nC/μF; $V_{1/2} = 12, 18.6, 21.4$ mV; $k = 15.5, 14.9, 10.4$ mV for β2a, β2-3′t, β2-3′t2; and (*C*) $Q_{max} = 5.4, 3.8$ nC/μF; $V_{1/2} = 25.8, 19.4$ mV; $k = 14, 10.5$ mV for β2-β1 and β2-β1-3′t transfected cells, respectively. The curve without symbols is a fit of *Q-V* curve of nontransfected cells ($Q_{max} = 2.5$ nC/μF; $V_{1/2} = -6$ mV; $k = 12$ mV).

The peak fluorescence at different voltages is shown in $\Delta F/F$ units in Fig. 8. The curves correspond to a Boltzmann fit of the population average $\Delta F/F$-*V* curves with parameters indicated in the figure legend. The curve without data corresponds to the fluo-3 fluorescence of nontransfected cells obtained in a previous study (Beurg et al., 1997). Averages of Boltzmann parameters fitted separately to each cell are shown in Table 1. All β constructs, without exception, recovered $\Delta F/F$-*V* curves that saturated at large positive potentials. This is expected of skeletal-type EC coupling but not of Ca^{2+}-entry dependent (cardiac-type) EC coupling (Garcia and Beam, 1994b). A bell-shaped $\Delta F/F$-*V* curve, indicative of cardiac-type EC coupling, was restored by coexpression of the cardiac isoform α_{1C} and wt β1a using the same pulse protocol and confocal imaging technique (Ahern et al., 1999). The recovery of skeletal EC coupling by the β constructs is entirely consistent with a recovery of DHPRs that include α_{1S}, a conclusion reached earlier by analyses of the voltage-dependence and kinetics of the recovered Ca^{2+} current. Deletion analyses of β1a in Fig. 8 *A* indicated that removal of region 3 (construct β1c) did not alter the maximum amplitude of Ca^{2+} transients reached at positive potentials. However, a significant decrease in the maximum $\Delta F/F$ was produced by removal of the C-terminus (construct β1a-3′t) or by partial removal of the N-terminus (construct β1a-5′t) of β1a.

As shown in Table 1, averages of several cells indicated a fivefold reduction in maximum $\Delta F/F$ in the former case (3.3/0.65) and a 1.7-fold in the latter case (3.3/1.9) with high statistical significance in both cases (unpaired *t*-tests with $p = 0.0002$ and 0.05, respectively). Because the Q_{max} recovered by each of the two constructs was not significantly different from that recovered by wt β1a (unpaired *t*-test, $p > 0.2$), the reduction in voltage-evoked Ca^{2+} release could not be explained by a reduction in the amount of DHPR complexes present in the cell surface of these myotubes. More likely, the deleted regions were necessary for the EC coupling function of the DHPR. In Fig. 8 *B* we investigated whether the low EC coupling produced by wt β2a was related to the C-terminus of β2a, which has a unique composition and is much larger in mass than region 5 of β1a. The deletion of 115 amino acids from the C-terminus of β2a (construct β2a-3′t) resulted in a 1.8-fold restoration (2.0/1.1) of $\Delta F/F_{max}$ that was marginally significant compared to that produced by wt β2a (unpaired *t*-test with $p = 0.06$). This increase in $\Delta F/F_{max}$ was consistent with the partial restoration of Q_{max} produced by the same construct, and suggested that the C-terminus of β2a could interfere with either the targeting of DHPRs to the cell surface, or EC coupling, or both. However, further C-truncation of 70 amino acids (construct β2a-3′t2) did not increase $\Delta F/F_{max}$. In fact, the opposite was the case as $\Delta F/F_{max}$ of β2a-3′t2 was less than that of β2a-3′t, although the difference was not significant (unpaired *t*-test with $p = 0.18$). The loss in activity produced by the deeper truncation could be caused by incorrect protein folding, because in this region there is a partially conserved α helix/β strand motif that was removed by the deletion (Hanlon et al., 1999).

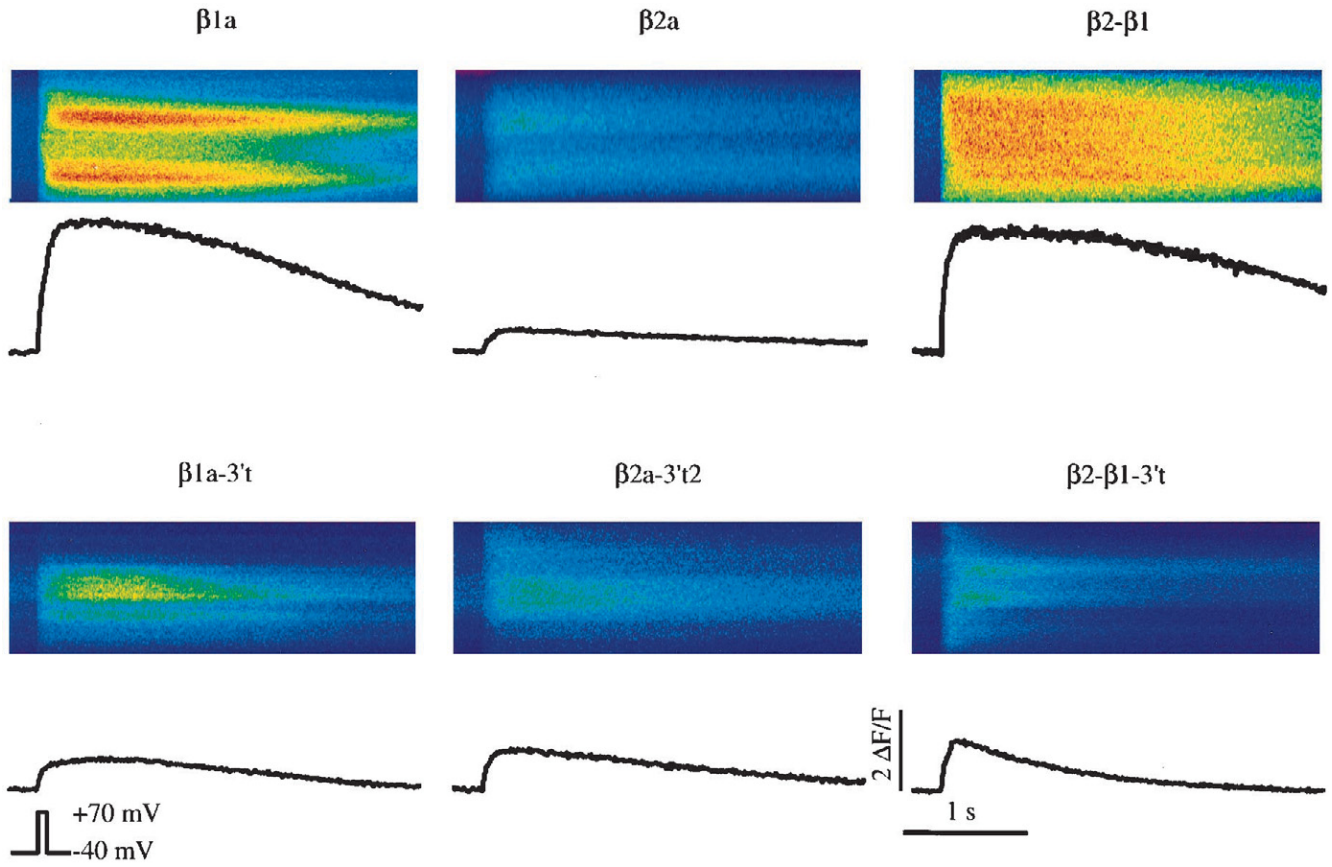

FIGURE 7 Confocal line-scan images of fluo-3 fluorescence in response to a 50-ms pulse to +70 mV from a holding potential of −40 mV. The curves show the time course of the normalized fluorescence intensity ($\Delta F/F$) obtained by integration of the image fluorescence. Images have a dimension of 2.05 s (horizontal) and 45, 42.5, 21.5, 43, 28.5, 73.7 μm for β1a, β1-3′t, β2a, β2-3′t2, β2-β1, and β2-β1-3′t, respectively.

Fig. 8 *C* shows that the β2-β1 chimera fully restored the $\Delta F/F_{max}$ present in cells expressing wt β1a. This indicated that the N-terminal half of β1a was interchangeable with that of β2a, and thus presumably the C-terminus half of β1a was specifically required for enhancing EC coupling. If this were the case, the C-terminus truncation of the chimera should produce the same result as the C-terminus truncation of wt β1a. This result is also shown in Fig. 8 *C*. The $\Delta F/F_{max}$ of the β2-β1-3′t truncated chimera was reduced 2.7-fold (3.8/1.4) compared to that produced by the "full-length" chimera, and the difference was statistically significant (unpaired *t*-test with $p = 0.005$). In summary, the confocal imaging of Ca^{2+} transients in β1-null cells expressing β constructs demonstrated that 1) the linker region 3 of β1a is nonessential for skeletal-type EC coupling; 2) a domain of the β1a subunit, near the C-terminus (region 5), and the N-terminus (region 1) strengthened skeletal-type EC coupling but did not affect Q_{max}; 3) a domain of the β2a subunit, also near the C-terminus (region 5), weakened EC coupling; and 4) the N-terminus half of β1a could be interchanged with the N-terminus half of β2a without a loss in the strength of EC coupling as determined by the maximum amplitude of Ca^{2+} transients.

DISCUSSION

We previously showed that full-length β1a or β2a expressed in β1-null cells became integrated into functional skeletal-type DHPR complexes that include α_{1S}, β1a or β2a, and presumably α_2-δ and γ subunits. This conclusion was based on many similar characteristics of the expressed DHPRs such as the Ca^{2+} current density and voltage-dependence, the slow kinetics of activation of the Ca^{2+} current, and estimations of the single channel currents based on nonstationary variance analyses (Beurg et al., 1999b). Critical differences between β1a and β2a were observed in the characteristics of the recovered EC coupling, which suggested that β2a was incapable of fully substituting for β1a as a component of the voltage sensor that triggers the Ca^{2+} transient. In the present study we used deletion mutants and chimeras of β1a and β2a to determine the molecular basis for 1) the ability of β1a to recover EC coupling when expressed in β1-null cells; and 2) the inability of β2a to recover charge movements and EC coupling with normal characteristics in the same cells. We identified the participation of the N- and C-termini of β1a in skeletal-type EC coupling and the interference of the C-terminus of β2a in the same process.

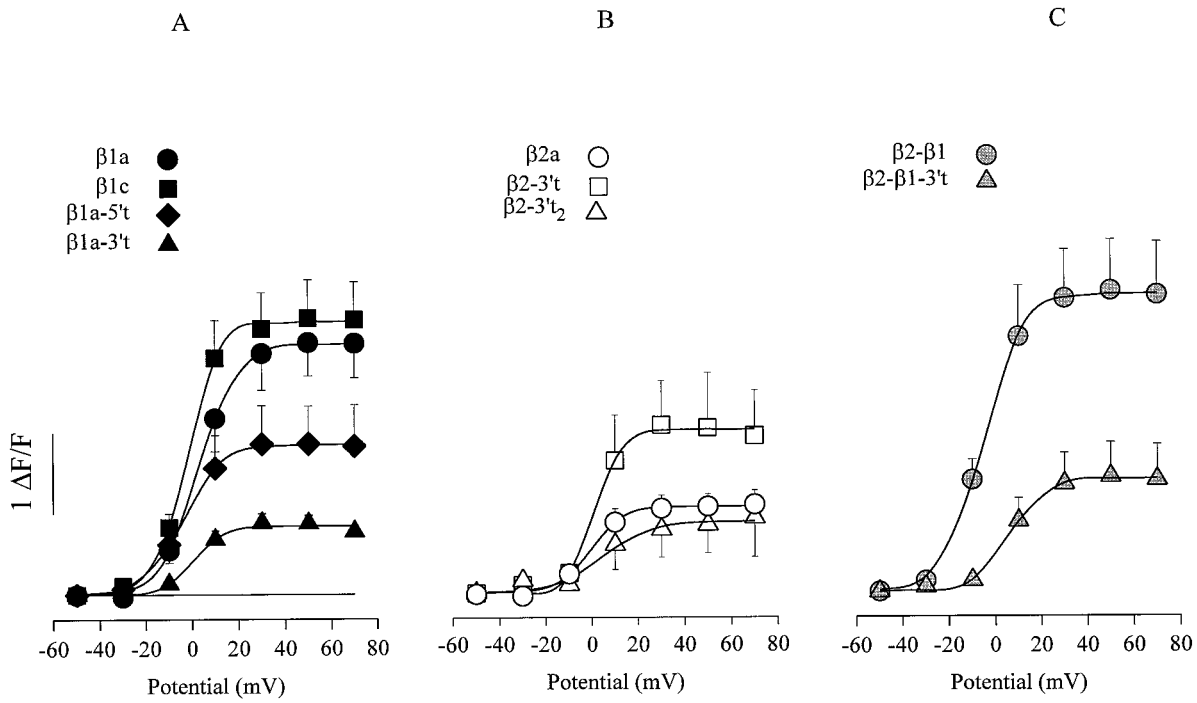

FIGURE 8 Ca^{2+} transients were elicited by 50-ms voltage steps to the indicated potential from a holding potential of −40 mV. $\Delta F/F$ at the peak of the transient (population mean ± SE) was obtained by integration of the confocal line-scan images. Curves correspond to Boltzmann fit of the population mean $\Delta F/F$-V curve. Parameters of the fit are (*A*) $\Delta F/F_{max}$ = 3.1, 3.4, 1.8, 0.8; $V_{1/2}$ = 3, −2.4, −4.1, 0.8 mV; k = 8.2, 6.8, 8.3, 6.4 mV for β1a (n = 9), β1c (n = 11), β1-5′t (n = 6), and β1-3′t (n = 3), respectively; (*B*) $\Delta F/F_{max}$ = 1, 2, 0.9; $V_{1/2}$ = −0.6, 1.5, 4.5 mV; k = 7, 5.8, 10.3 mV for β2a (n = 7), β2-3′t (n = 4), β2-3′t2 (n = 6); and (*C*) $\Delta F/F_{max}$ = 3.7, 1.4; $V_{1/2}$ = −5.4, 6.3 mV; k = 8.4, 7.6 mV for β2-β1 (n = 7) and β2-β1-3′t (n = 10) transfected cells, respectively.

Because the N-terminus of β1a and β2a have amino acid sequences that are entirely divergent, yet the N-terminus half of β2a supported EC coupling, the N-terminus of β1a was a far less critical determinant of EC coupling than the C-terminus of β1a. Since a domain of the pore-forming α_{1S} subunit is also required for EC coupling in skeletal myotubes (Nakai et al., 1998b), the present observations suggest two distinct hypotheses. The identified C-terminal region of β1a could either assist α_{1S}, or function in parallel with α_{1S}, to bring about EC coupling with normal characteristics. For example, the identified domain could bring about a close colocalization of DHPRs and RyRs across from the junctional membrane that would enable α_{1S} to signal opening of the RyR. Alternatively, the identified domain could be an element of the signal that opens the RyRs. These two possibilities, although seemingly dissimilar, may represent two manifestations of the same molecular interaction between β and the RyR or between β and other junctional proteins.

The deletion analyses of the present study indicated that the nonhomologous C-termini of β1a and β2a have significant consequences for the EC coupling function of the DHPR. However these two peptidic regions produced nonequivalent effects. Removal of the β1-specific C-terminus had no effect on charge movements and reduced the Ca^{2+} transients, whereas removal of the β2-specific C-terminus lead to an increase in the expression of charge movement and to a dual effect on Ca^{2+} transients. There was an increase in $\Delta F/F_{max}$ in cells expressing β2a-3′t followed by a decrease in $\Delta F/F$ in cells expressing the more drastic truncation (β2a-3′t2). The C-terminal region of β2a is ~115 amino acids longer than that of β1a, and is predicted to be more hydrophilic (higher Kyte-Doolittle index) and more flexible (higher Karplus-Schulz index) than that of β1a. The β2a-specific region could represent an unusually active surface for interactions with cytoplasmic proteins, including secondary interactions with the cytoplasmic loops of the α_{1S} subunit, which could have inhibited charge movements and disrupted normal EC coupling. There is also the distinct possibility, based on the fact that β enhances transport of Ca^{2+} channels to the cell surface (Chien et al., 1995), that a β1-specific event may be required for transport of α_{1S}/β1 channels to the cell surface, whereas α_{1S}/β2 channels were prevented from reaching the cell surface. This could explain the fact that EC coupling was only partially restored by the combined expression of α_{1S} and β2 and that charge movements expressed by β2a were undetectable. However, this explanation has to be confronted with the additional experimental fact that the three β2 constructs tested express Ca^{2+} currents with a normal (wt) density and slow kinetics characteristics of skeletal L-type Ca^{2+} channels. Recent studies have shown that RyRs facilitate the expression of the normal L-type Ca^{2+} current density by a mechanism likely to involve a retrograde signal

from the RyR to the DHPR (Nakai et al., 1996). Consequently, one would have to assume that β2a-expressing cells have a normal (wt) density of DHPRs on the cell surface. Fluorescent tagging of Ca^{2+} channel subunits α_{1S} and β isoforms should further provide critical information on this issue.

It is entirely conceivable that the C-terminus of β1a could participate in EC coupling signaling, the event that opens the RyR. However, the comparatively small size of β1a would necessitate, in this case, that DHPRs and RyRs be in close proximity. The evidence in favor of a physical coupling of DHPRs and RyRs is overwhelmingly supportive and includes 1) the identification of the skeletal DHPR II-III loop as an essential component of the EC coupling (Tanabe at al., 1990; Adams et al., 1990; Nakai et al., 1998b); 2) functional interactions between II-III loop peptides and RyRs (El-Hayek et al., 1995); 3) coprecipitation of solubilized DHPR and RyRs (Marty et al., 1994); 4) interaction of II-III loop fragments and RyR fragments (Leong et al., 1998a, b); and 5) a recent identification of a domain in the RyR that is specifically required for expression of L-type Ca^{2+} current by the DHPR (Nakai et al., 1998a). The latter evidence is particularly compelling because skeletal-type Ca^{2+} channel expression is poor in nonmuscle cells, even in a highly efficient system such as the amphibian oocyte (Ren and Hall, 1997). Interactions between the Ca^{2+} channel β subunit and the RyR are entirely speculative, although in a tightly coupled multisubunit system it is entirely reasonable to suspect these interactions may be present. We surmise that in the assembled Ca^{2+} channel all the cytosolic loops of α_{1S} must be brought close to each other in the space under the cytoplasmic face of the channel. Because β binds strongly to the I-II loop of α_{1S}, it is almost impossible for this subunit not to be in close contact with the II-III loop of α_{1S} and the RyR1. Consequently, domains of β could form a complex with the II-III loop and the RyR1. These potentially significant interactions clearly deserve further investigation.

The present studies agree with some, but not all, previously proposed functions of β subunits inferred from studies in heterologous expression systems. These studies have shown that the interaction of α_1 and β subunits affects the gating of the expressed Ca^{2+} channel and, at the same time, is required for the stabilization of the Ca^{2+} channel at the cell membrane. Coexpression of α_1 and β isoforms results, in most cases, in Ca^{2+} currents with a higher density and faster kinetics (Olcese et al., 1994; Quin et al., 1996; Jones et al., 1998). In addition, β subunits facilitate gating of the Ca^{2+} channel by increasing the coupling between charge movement and pore opening (Neely et al., 1993; Olcese et al., 1996) although exceptions have been described (Josephson and Varadi, 1996; Kamp et al., 1996).

In oocytes it was shown that the N-terminus (region 1) of β is a critical determinant of the rate and voltage at which α_{1E} Ca^{2+} channels activate (Olcese et al., 1994). A second domain that includes the linker region 3 was shown to affect inactivation by a mechanism independent of that affecting activation (Quin et al., 1996). A more recent study in HEK cells, aiming to identify the molecular basis of the transport function of the β2a subunit, showed that neither region 1 nor 5 was essential for the surface expression of α_{1C} Ca^{2+} channels nor for expression of DHP binding sites accessible from the outside of the cell (Gao et al., 1999). Studies in oocytes have indicated that endogenous low-level expression of β3 is sufficient for the transport function, whereas a robust overexpression of exogenous β3 was required for affecting the gating of coexpressed α_{1E} Ca^{2+} channels (Tareilus et al., 1997). Thus, it has been suggested that modulation of gating is produced by low-affinity binding sites on the α_1 subunit occupied by overexpressed β, whereas the Ca^{2+} channel transport function only appears to require the higher-affinity AID/BID interaction (Tareilus et al., 1997; Neuhuber et al., 1998b; Gao et al., 1999).

There are several observations obtained here in β-null cells pertinent to the gating and transport functions of β. First, the present studies showed that the C-terminus region of β1 is a critical determinant of the EC coupling function of the DHPR, a region not previously correlated with any known gating or transport function of β. This finding highlights the need for homologous expression systems for understanding cell-specific functions of Ca^{2+} channels. Second, our finding of a lack of modulation of the Ca^{2+} channel conductance versus voltage relationship and activation kinetics by the various β constructs suggests that, in skeletal myotubes, α_{1S} and not β was the overwhelming determinant of the gating characteristics of the Ca^{2+} channel. Finally, because all β constructs tested had intact BID regions and expressed high-density L-type Ca^{2+} currents, the present results are entirely consistent with the appraisal of the AID/BID interaction as a major, and perhaps the only, structural determinant required for the surface expression of the Ca^{2+} channel. This conclusion is consistent with the lack of correlation between the recovery of the L-type Ca^{2+} current density and EC coupling (see Table 1), which suggests that both functions are indeed regulated by different structural domains in the β subunit. It is possible that subpopulations of Ca^{2+} channels could be separately responsible for the L-type Ca^{2+} current and EC coupling. These subpopulations could originate from post-translational processing of the β construct (Chien et al., 1995) and could account for the lack of correlation of the biophysical parameters listed in Table 1.

This work was supported by National Institutes of Health Grant HL-47053 (to R.C., P.A.P., and R.G.G.).

REFERENCES

Adams, B. A., T. Tanabe, A. Mikami, S. Numa, and K. G. Beam. 1990. Intramembrane charge movement restored in dysgenic skeletal muscle by injection of dihydropyridine receptor cDNAs. *Nature*. 346:569–572.

Ahern, C., P. A. Powers, R. Gregg, and R. Coronado. 1999. Expression of cardiac DHPR α1C in $\alpha1^{-}/\beta1^{-}$ double mutant skeletal muscle myotubes. *Biophys. J.* 76:467*a* (Abstr.).

Beurg, M., C. Ahern, P. A. Powers, R. Gregg, and R. Coronado. 1999a. Domain of the calcium channel β1 subunit involved in excitation-contraction coupling. *Biophys. J.* 76:394*a* (Abstr.).

Beurg, M., C. Sukhareva, M. W. Ahern, J. A. Conklin, C. Powell, P. A. Powers, R. G. Gregg, and R. Coronado, R. 1999b. Differential control of skeletal muscle Ca^{2+} current and excitation-contraction coupling by the dihydropyridine receptor β subunit. *Biophys. J.* 76:1744–1756.

Beurg, M., M. Sukhareva, C. Strube, P. A. Powers, R. G. Gregg, and R. Coronado. 1997. Recovery of Ca^{2+} current, charge movements, and Ca^{2+} transients in myotubes deficient in dihydropyridine receptor β_1 subunit transfected with β_1 cDNA. *Biophys. J.* 73:807–818.

Block, B. A., T. Imagawa, K. P. Campbell, and C. A. Franzini-Armstrong. 1988. Structural evidence for direct interaction between the molecular components of the transverse tubule/sarcoplasmic reticulum junction in skeletal muscle. *J. Cell Biol.* 107:2587–2600.

Chaudhari, N., and K. G. Beam. 1993. mRNA for cardiac calcium channel is expressed during development of skeletal muscle. *Dev. Biol.* 155: 507–515.

Chien, A. J., X. L. Zhao, R. E. Shirokov, T. S. Puri, C. F. Chang, D. Sun, E. Rios, and M. M. Hosey. 1995. Roles of a membrane-localized beta subunit in the formation and targeting of functional L-type Ca^{2+} channels. *J. Biol. Chem.* 270:30036–30044.

Conklin, M., P. Powers, R. G. Gregg, and R. Coronado. 1999. Ca^{2+} sparks in embryonic mouse skeletal muscle selectively deficient in dihydropyridine receptor α1S or β1 subunits. *Biophys. J.* 76:657–669.

Craven, S. E., and D. S. Bredt. 1998. Minireview: PDZ proteins organize synaptic signaling pathways. *Cell*. 93:495–498.

De Waard, M., M. Pragnell, and P. K. Campbell. 1994. Ca^{2+} channel regulation by a conserved β subunit domain. *Neuron*. 13:495–503.

Dirksen, R. T., and K. G. Beam. 1995. Single calcium channel behavior in native skeletal muscle. *J. Gen. Physiol.* 105:227–247.

Ebashi, S., M. Endo, and I. Oktsuki. 1969. Control of muscle contraction. *Q. Rev. Biophys.* 2:351–384.

El-Hayek, R., B. Antoniu, J. Wang, S. L. Hamilton, and N. Ikemoto. 1995. Identification of a calcium release-triggering and blocking regions of the II-III loop of the skeletal muscle DHPR. *J. Biol. Chem.* 270: 22116–22118.

Gao, T., A. J. Chien, and M. M. Hosey. 1999. Complexes of the α1C and β subunits generate the necessary signal for membrane targeting of class C L-type calcium channels. *J. Biol. Chem.* 274:2137–2144.

Garcia, J., T. Tanabe, and K. G. Beam. 1994a. Relationship of calcium transients to calcium currents and charge movements in myotubes expressing skeletal and cardiac dihydropyridine receptors. *J. Gen. Physiol.* 103:125–147.

Garcia, J., and K. G. Beam. 1994b. Measurement of calcium transients and slow calcium current in myotubes. *J. Gen. Physiol.* 103:107–123.

Gregg, R. G., A. Messing, C. Strube, M. Beurg, R. Moss, M. Behan, M. Sukhareva, S. Haynes, J. A. Powell, R. Coronado, and P. Powers. 1996. Absence of the β subunit (*cchβ1*) of the skeletal muscle dihydropyridine receptor alters expression of the α_1 subunit and eliminates excitation-contraction coupling. *Proc. Natl. Acad. Sci. USA.* 93:13961–13966.

Hanlon, M. R., N. S. Berrow, A. C. Dolphin, and B. A. Wallace. 1999. Modelling of a voltage-dependent Ca^{2+} channel β subunit as a basis for understanding its functional properties. *FEBS Lett.* 445:366–370.

Jones, L. P., A-K. Wei, and D. T. Yue. 1998. Mechanism of auxiliary subunit modulation of α1E calcium channels. *J. Gen. Physiol.* 112:125–143.

Josephson, I. R., and G. Varadi. 1996. The β subunit increases Ca^{2+} currents and gating charge movements of human cardiac L-type Ca^{2+} channels. *Biophys. J.* 70:1285–1293.

Kamp, T., M. T. Perez-Garcia, and E. Marban. 1996. Enhancement of ionic current and charge movement by coexpression of calcium channel β_{1a} subunit with α_{1C} subunit in a human embryonic kidney cell line. *J. Physiol.* 492:89–96.

Leong, P., and D. H. MacLennan. 1998a. A 37-amino acid sequence in the skeletal muscle ryanodine receptor interacts with the cytoplasmic loop between domain II and domain III in the skeletal muscle dihydropyridine receptor. *J. Biol. Chem.* 273:7791–7794.

Leong, P., and D. H. MacLennan. 1998b. The cytoplasmic loops between domains II and III and domains III and IV in the skeletal muscle dihydropyridine receptor bind to a contiguous site in the skeletal muscle ryanodine receptors. *J. Biol. Chem.* 273:29958–29964.

Leung, A. T., T. Imagawa, and K. P. Campbell. 1987. Structural characterization of the 1,4-dihydropyridine receptor of the voltage-gated Ca^{2+} channel from rabbit skeletal muscle. *J. Biol. Chem.* 262:7943–7946.

Marty, I., M. Robert, M. Villaz, K. S. DeJongh, Y. Lai, W. A. Catterall, and M. Ronjat. 1994. Biochemical evidence for a complex involving dihydropyridine receptor and ryanodine receptor in triad junctions of skeletal muscle. *Proc. Natl. Acad. Sci. USA.* 91:2270–2274.

Nakai, J., R. T. Dirksen, H. T. Nguyen, I. N. Pessah, K. G. Beam, and P. D. Allen. 1996. Enhanced dihydropyridine channel activity in the presence of ryanodine receptor. *Nature.* 380:72–75.

Nakai, J., N. Sekiguchi, T. A. Rando, P. D. Allen, and K. G. Beam. 1998a. Two regions of the ryanodine receptor involved in coupling with L-type Ca^{2+} channels. *J. Biol. Chem.* 273:13403–13406.

Nakai, J., T. Tanabe, T. Konno, B. Adams, and K. G. Beam. 1998b. Localization in the II-III loop of the dihydropyridine receptor of a sequence critical for excitation-contraction coupling. *J. Biol. Chem.* 273:24983–24986.

Neely, A., X. Wei, R. Olcese, L. Birnbaumer, and E. Stefani. 1993. Potentiation by the β subunit of the ratio of the ionic current to the charge movement in the cardiac calcium channel. *Science.* 262:575–578.

Neuhuber, B., U. Gerster, F. Doring, H. Glossmann, T. Tanabe, and B. E. Flucher. 1998b. Association of calcium channel α1s and β1a subunits is required for the targeting of β1a but not of α1S into skeletal muscle triads. *Proc. Natl. Acad. Sci. USA.* 95:5015–5020.

Olcese, R., A. Neely, N. Qin, X. Wei, L. Birnbaumer, and E. Stefani. 1996. Coupling between charge movement and pore opening in vertebrate neuronal α_{1E} calcium channels. *J. Physiol.* 497.3:675–686.

Olcese, R., N. Qin, T. Schneider, A. Neely, X. Wei, E. Stefani, and L. Birnbaumer. 1994. The amino terminus of a calcium channel β subunit sets rates of channel inactivation independently of the subunit's effect on activation. *Neuron*. 13:1433–1438.

Pereon, Y., J. Navarro, and P. T. Palade. 1997. Expression of the dihydropyridine receptor alpha-1C subunit isoforms in adult rat and mouse skeletal muscle. *Biophys. J.* 72:149*a* (Abstr.).

Perez-Reyes, E., and T. Schneider. 1994. Calcium channels: Structure, function, and classification. *Drug Dev. Res.* 33:295–318.

Powers, P. A., S. Liu, K. Hogan, and R. G. Gregg. 1992. Skeletal muscle and brain isoforms of a β subunit of human voltage-dependent calcium channels are encoded by a single gene. *J. Biol. Chem.* 267:22967–22972.

Pragnell, M., M. De Waard, Y. Mori, T. Tanabe, T. P. Snutch, and K. P. Campbell. 1994. Calcium channel β-subunit binds to a conserved motif in the I-II cytoplasmic linker of the α_1-subunit. *Nature.* 368:67–70.

Quin, N., R. Olcese, J. Zhou, O. A. Cabello, L. Birnbaumer, and E. Stefani. 1996. Identification of a second region of the β-subunit involved in regulation of calcium channel inactivation. *Am. J. Physiol.* 271: C1539–C1545.

Ren, D., and L. M. Hall. 1997. Functional expression and characterization of skeletal muscle dihydropyridine receptors in *Xenopus* oocytes. *J. Biol. Chem.* 272:22393–22396.

Ruth, P., A. Rohrkasten, M. Biel, E. Bosse, S. Regulla, H. E. Meyer, V. Flockerzi, and F. Hofmann. 1989. Primary structure of the β subunit of the DHP-sensitive calcium channel from skeletal muscle. *Science.* 245: 1115–1118.

Scott, V. E. S., C. A. Gurnett, and K. P. Campbell. 1997. Overlay and bead assay. Determination of calcium channel subunit interaction domains. *In* Methods in Molecular Biology, Vol. 88: Protein Targeting Protocols. R. A. Clegg, editor. Humana Press Inc., Totowa, NJ.

Strube, C., M. Beurg, P. A. Powers, R. G. Gregg, and R. Coronado. 1996. Reduced Ca^{2+} current, charge movement and absence of Ca^{2+} transients in skeletal muscle deficient in dihydropyridine receptor β_1 subunit. *Biophys. J.* 71:2531–2543.

Strube, C., M. Beurg, C. Sukhareva, J. A. Ahern, C. Powell, P. A. Powers, R. G. Gregg, and R. Coronado. 1998. Molecular origin of the Ca^{2+} current of skeletal muscle myotubes selectively deficient in dihydropyridine receptor β_1 subunit. *Biophys. J.* 75:207–217.

Takekura, H., L. Bennett, T. Tanabe, K. G. Beam, and C. Franzini-Armstrong. 1994. Restoration of junctional tetrads in dysgenic myotubes by dihydropyridine receptor cDNA. *Biophys. J.* 67:793–803.

Tanabe, T., B. A. Adams, S. Numa, and K. G. Beam. 1991. Repeat I of the dihydropyridine receptor is critical in determining calcium channel activation kinetics. *Nature.* 352:800–803.

Tanabe, T., K. G. Beam, B. A. Adams, T. Niidome, and S. Numa. 1990. Regions of the skeletal muscle dihydropyridine receptor critical for excitation-contraction coupling. *Nature*. 346:567–572.

Tareilus, E., M. Roux, N. Qin, R. Olcese, J. Zhou, E. Stefani, and L. Birnbaumer. 1997. A *Xenopus* oocyte β subunit. Evidence for a role in the assembly/expression of voltage-gated calcium channels that is separate from its role as a regulatory subunit. *Proc. Natl. Acad. Sci. USA.* 94:1703–1708.

Wicher, D. R., M. De Waard, H. Liu, M. Pragnell, and K. P. Campbell. 1995. Association of native Ca^{2+} channel β subunits with the α1 subunit interaction domain. *J. Biol. Chem.* 270:18088–18093.